

# Dihadron Tomography of High-Energy Nuclear Collisions in NLO pQCD

Hanzhong Zhang<sup>a</sup>, J. F. Owens<sup>b</sup>, Enke Wang<sup>a</sup> and Xin-Nian Wang<sup>c</sup>

<sup>a</sup>*Institute of Particle Physics, Huazhong Normal University, Wuhan 430079, China*

<sup>b</sup>*Physics Department, Florida State University, Tallahassee, FL 32306-4350, USA*

<sup>c</sup>*Nuclear Science Division, Lawrence Berkeley Laboratory, Berkeley, California 94720, USA*

Back-to-back dihadron spectra in high-energy heavy-ion collisions are studied within the next-to-leading order (NLO) perturbative QCD parton model with jet quenching incorporated via modified jet fragmentation functions due to radiative parton energy loss in dense medium. The experimentally observed appearance of back-to-back dihadrons at high  $p_T$  is found to originate mainly from jet pairs produced close and tangential to the surface of the dense matter. However, a substantial fraction of observed high  $p_T$  dihadrons also comes from jets produced at the center of the medium after losing finite amount of energy. Consequently, the suppression factor of such high- $p_T$  hadron pairs is found to be more sensitive to the initial gluon density than the single hadron spectra that are dominated by surface emission. A simultaneous  $\chi^2$ -fit to both the single and dihadron spectra can be achieved within a narrow range of the energy loss parameters  $\epsilon_0 = 1.6 - 2.1$  GeV/fm. Because of the flattening of the initial jet production spectra, high  $p_T$  dihadrons at the LHC energy are found to be more robust as probes of the dense medium.

PACS numbers: 12.38.Mh, 24.85.+p; 25.75.-q

Jet quenching as discovered in high-energy heavy-ion collisions at the Relativistic Heavy-ion Collider (RHIC) is manifested in both the suppression of single inclusive hadron spectra at large transverse momentum ( $p_T$ ) [1] and the disappearance of the typical back-to-back jet structure in dihadron correlation in vacuum [2]. Since jet quenching is caused by parton energy loss which in turn depends on the gluon density and transport coefficient of the medium, detailed study of the suppression of large  $p_T$  hadron spectra and correlations can shed light on the properties of the dense medium [3].

In heavy-ion collisions, the spatial distribution of the initial jet production points is given by the nuclear overlap,  $T_{AB}(\mathbf{b}, \mathbf{r}) = t_A(r)t_B(|\mathbf{b} - \mathbf{r}|)$  with  $t_A(r)$  being the thickness function of each nucleus. The suppression factor of the leading hadrons from jet fragmentation will depend on the total parton energy loss which in turn is related to the weighted gluon density integrated along the jet propagation path. Therefore, measurements of large  $p_T$  hadron suppression can be directly related to the averaged gluon density and medium transport coefficient. As the average gluon density increases with colliding energy and centrality, one should expect continued decrease of the suppression factor until it reaches the limit of surface emission in the outer corona of the medium [4]. Once this limit is approached, the suppression factor of high- $p_T$  hadron spectra will lose its effectiveness as a sensitive probe since it only depends on the thickness of the outer corona which varies very slowly with the initial gluon density. In this Letter we will employ for the first time a next-to-leading order (NLO) perturbative QCD (pQCD) parton model to study the suppression of both single and dihadron spectra due to jet quenching. In particular, we will investigate the robustness of back-to-back dihadron spectra as a probe of the initial gluon density when single hadron spectra suppression become fragile.

Within the NLO pQCD parton model, large  $p_T$  hadron

production cross section in  $p + p$  collisions can be expressed as a convolution of NLO parton-parton scattering cross sections, parton distributions inside nucleons and parton fragmentation functions (FF). The calculations discussed in this Letter are carried out within a NLO Monte Carlo based program [5] which utilizes two-cutoff parameters,  $\delta_s$  and  $\delta_c$ , to isolate the soft and collinear divergences in the squared matrix elements of the  $2 \rightarrow 3$  processes. The regions containing the divergences are integrated over in  $n$ -dimensions and the results are combined with the squared matrix elements for the  $2 \rightarrow 2$  processes. This results in a set of two-body and three-body weights, each of which depends on the cut-offs. However, this dependence cancels when the weights are combined in the calculation of physical observables.

For the study of large  $p_T$  single and dihadron production in  $A + A$  collisions, we assume that the initial hard scattering cross sections are factorized as in  $p + p$  collisions. As in the lowest-order (LO) pQCD parton model study [6], we further assume that the effect of final-state interaction between produced parton and the bulk medium can be described by the effective medium-modified FF's,

$$D_{h/c}(z_c, \Delta E_c, \mu^2) = (1 - e^{-\langle \frac{L}{\lambda} \rangle}) \left[ \frac{z'_c}{z_c} D_{h/c}^0(z'_c, \mu^2) + \langle \frac{L}{\lambda} \rangle \frac{z'_g}{z_c} D_{h/g}^0(z'_g, \mu^2) \right] + e^{-\langle \frac{L}{\lambda} \rangle} D_{h/c}^0(z_c, \mu^2), \quad (1)$$

where  $z'_c = p_T/(p_{Tc} - \Delta E_c)$ ,  $z'_g = \langle L/\lambda \rangle p_T/\Delta E_c$  are the rescaled momentum fractions,  $\Delta E_c$  is the average radiative parton energy loss and  $\langle L/\lambda \rangle$  is the number of scatterings. The FF's in vacuum  $D_{h/c}^0(z_c, \mu^2)$  are given by the KKP parameterization [7].

According to recent theoretical studies [8, 9, 10] the total parton energy loss in a finite and expanding medium

can be approximated as a path integral,

$$\Delta E \approx \langle \frac{dE}{dL} \rangle_{1d} \int_{\tau_0}^{\infty} d\tau \frac{\tau - \tau_0}{\tau_0 \rho_0} \rho_g(\tau, \mathbf{b}, \mathbf{r} + \mathbf{n}\tau), \quad (2)$$

for a parton produced at a transverse position  $\mathbf{r}$  at an initial time  $\tau_0$  and traveling along the direction  $\mathbf{n}$ .  $\langle dE/dL \rangle_{1d}$  is the average parton energy loss per unit length in a 1-d expanding medium with an initial uniform gluon density  $\rho_0$  at  $\tau_0$ . The energy dependence of the energy loss is parameterized as

$$\langle \frac{dE}{dL} \rangle_{1d} = \epsilon_0 (E/\mu_0 - 1.6)^{1.2} / (7.5 + E/\mu_0), \quad (3)$$

from the numerical results in Ref. [9] in which thermal gluon absorption is also taken into account. The parameter  $\epsilon_0$  should be proportional to  $\rho_0$ .

Neglecting transverse expansion, the gluon density distribution in a 1-d expanding medium in  $A + A$  collisions at impact-parameter  $\mathbf{b}$  is assumed to be proportional to the transverse profile of participant nucleons ,

$$\rho_g(\tau, \mathbf{b}, \mathbf{r}) = \frac{\tau_0 \rho_0}{\tau} \frac{\pi R_A^2}{2A} [t_A(\mathbf{r}) + t_A(|\mathbf{b} - \mathbf{r}|)]. \quad (4)$$

The average number of scatterings along the parton propagating path is

$$\langle L/\lambda \rangle = \int_{\tau_0}^{\tau_0+L} \frac{d\tau}{\rho_0 \lambda_0} \rho_g(\tau, \mathbf{b}, \mathbf{r} + \mathbf{n}\tau). \quad (5)$$

Here, we neglect the time-dependence of the cross section and characterize it by the mean free path  $\lambda_0$  via  $\sigma_0 = 1/(\rho_0 \lambda_0)$  and a hard-sphere nuclear distribution is used. The parton distributions per nucleon  $f_{a/A}(x_a, \mathbf{r})$  inside the nucleus are assumed to be factorizable into the parton distributions in a nucleon given by CTEQ6M parameterization [11] and the new HIJING parameterization [12] of the impact-parameter dependent nuclear modification factor, including the isospin dependence.

The calculated single inclusive  $\pi^0$  and  $\pi^+ + \pi^-$  spectra in the NLO pQCD parton model in  $p + p$  collisions agree well with the experimental data at the RHIC energy with the factorization scale in the range  $\mu = 0.9 \sim 1.5 p_T$  [13]. We use the same factorization scale in both  $p + p$  and  $A + A$  collisions in our calculation. Shown in Fig. 1 are the nuclear modification factors,

$$R_{AA} = \frac{d\sigma_{AA}/dp_T^2 dy}{\int d^2b T_{AA}(\mathbf{b}) d\sigma_{NN}/dp_T^2 dy}, \quad (6)$$

for the single inclusive  $\pi^0$  spectra calculated in both leading-order (LO) and NLO pQCD parton model as compared to the PHENIX data on central  $Au + Au$  collisions at  $\sqrt{s} = 200$  GeV. The factorization scale in the NLO result is set  $\mu = 1.2 p_T$  though the nuclear modification factor  $R_{AA}$  is not at all sensitive to the choice of  $\mu$ . However,  $R_{AA}$  in NLO calculation is always smaller than the LO result at high  $p_T$  because of the relative larger

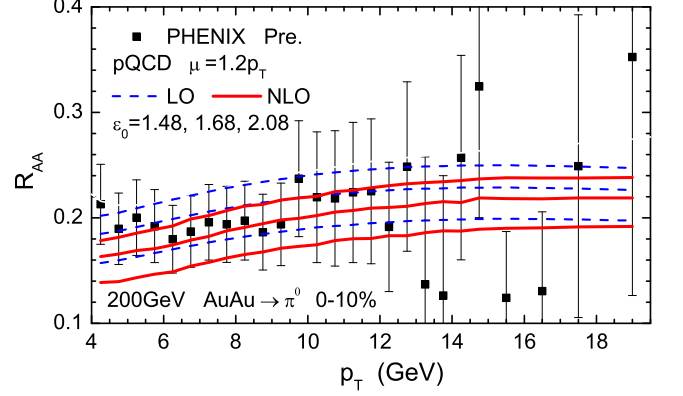


FIG. 1: Nuclear modification factors for  $\pi^0$  spectra in LO (dashed) and NLO pQCD (solid) in  $Au + Au(0 - 10\%)$  collisions at  $\sqrt{s} = 200$  GeV with different values of energy loss parameter  $\epsilon_0 = 1.48, 1.68$  and  $2.08$  GeV/fm (from top to bottom) compared with data [14].

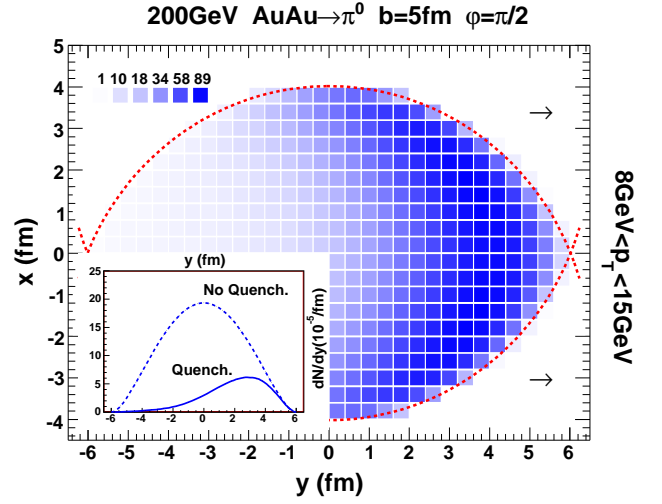


FIG. 2: Spatial transverse distribution (arbitrary normalization) of the initial parton production points that contribute to the final  $\pi^0$  at  $8 < p_T < 15$  GeV along  $\phi = \pi/2$ . The insert is the same distribution projected onto the  $y$ -axis.

ratio of gluon/quark jets in NLO than in LO calculation and gluon energy loss is assumed to be 9/4 larger than that of a quark. In both calculations, we have chosen the parameters as  $\mu_0 = 1.5$  GeV and  $\epsilon_0 \lambda_0 = 0.5$  GeV.

Because of jet quenching, the dominant contribution to the measured single hadron spectra at large  $p_T$  comes from those jets that are initially produced in the outer corona of the overlap region toward the direction of the detected hadron. This is clearly illustrated in Fig. 2 by the spatial distribution of the production points of those jets that have survived the interaction with the medium and contribute to the measured spectra. Jets produced in the region away from the detected hadron are severely suppressed due to their large energy loss and don't contribute much to the final hadron spectra. As pointed

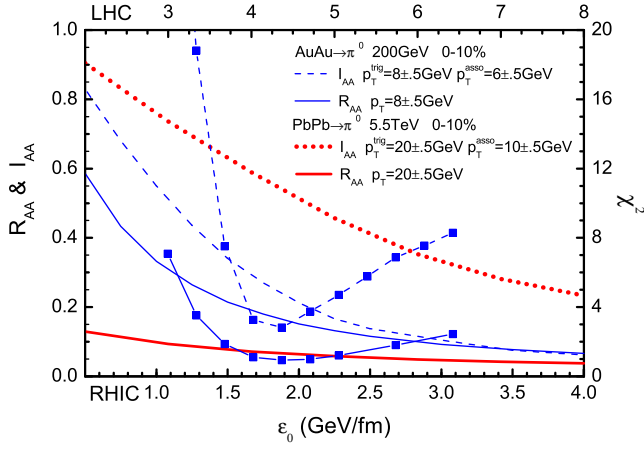


FIG. 3: The suppression factors for single ( $R_{AA}$ ) and di-hadron ( $I_{AA}$ ) spectra at fixed transverse momentum as functions of the initial energy loss parameter  $\epsilon_0$ . Also shown are  $\chi^2$ 's (curves with filled squares) in fitting experimental data on single [14] ( $p_T = 4 - 20$  GeV/c) and away-side spectra [15] ( $p_T^{\text{trig}} = 8 - 15$  GeV,  $z_T = 0.45 - 0.95$ ) in central Au + Au collisions at  $\sqrt{s} = 200$  GeV.

out in Ref. [4], when jets produced in the inner part of the overlapped region are completely suppressed due to large initial gluon density, the final large  $p_T$  hadron production is dominated by “surface emission”. However, high- $p_T$  hadron yield via such surface emission should be proportional to the thickness of the outer corona which decreases with the initial gluon density. Therefore, the suppression factor for single hadron spectra should never saturate but continue to decrease with the initial gluon density as shown in Fig. 3. The variation, nevertheless, is weak when surface emission becomes dominant and single hadron suppression might not be a sensitive probe of the initial gluon density.

To find robust probes of the high initial gluon density when single hadron spectra suppression becomes fragile, we will study back-to-back dihadron spectra within NLO pQCD parton model in this Letter. To quantify dihadron spectra, a hadron-triggered fragmentation function,

$$D_{AA}(z_T, p_T^{\text{trig}}) \equiv p_T^{\text{trig}} \frac{d\sigma_{AA}^{h_1 h_2} / dy^{\text{trig}} dp_T^{\text{trig}} dy^{\text{asso}} dp_T^{\text{asso}}}{d\sigma_{AA}^{h_1} / dy^{\text{trig}} dp_T^{\text{trig}}}, \quad (7)$$

was introduced [6] as a function of  $z_T = p_T^{\text{asso}} / p_T^{\text{trig}}$ , which is essentially the away-side hadron spectrum associated with a triggered hadron. Both hadrons are limited to the central rapidity region  $|y^{\text{trig,asso}}| < 0.5$  and the azimuthal angle relative to the triggered hadron is integrated over  $|\Delta\phi| > 2.5$ .

As in the NLO calculation of single hadron spectra, one also has to fix the factorization scale in the NLO calculation of dihadron spectra, which is chosen to be the invariant mass of the dihadron  $M^2 = (p_1 + p_2)^2$ . The NLO results on associated hadron spectra  $D_{pp}(z_T, p_T^{\text{trig}})$  in  $p+p$  collisions are compared to the  $d+Au$  data at  $\sqrt{s} =$

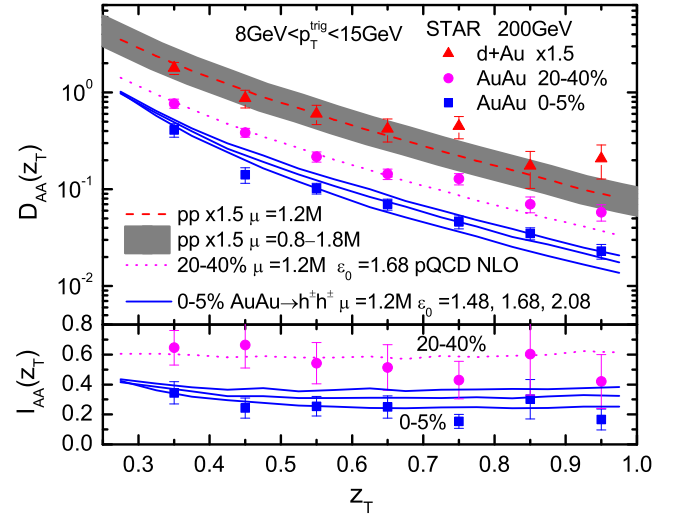


FIG. 4: Hadron-triggered fragmentation functions  $D_{AA}(z_T)$  and the medium modification factors  $I_{AA}(z_T)$  in NLO pQCD as compared to the data [15].

200 GeV in Fig. 4, assuming no nuclear effects in  $d + Au$  collisions. The overall normalization of NLO results is quite sensitive to the factorization scale as indicated by the shaded region corresponding to  $\mu = 0.8 - 1.8M$ . We will use  $\mu = 1.2M$  in this study with which NLO results describe the experimental data well. We use the same scale in the calculation of dihadron spectra in Au + Au collisions and the results for  $D_{AA}(z_T, p_T^{\text{trig}})$  agree well with STAR data as shown in Fig. 4 using the same energy loss parameter  $\epsilon_0 = 1.68 - 2.08$  GeV/fm. The centrality dependence of the data is also reproduced by the NLO calculation [13]. The nuclear modification factor of the hadron-triggered fragmentation function

$$I_{AA} = \frac{D_{AA}(z_T, p_T^{\text{trig}})}{D_{pp}(z_T, p_T^{\text{trig}})} \quad (8)$$

as plotted in the lower panel is coincidentally similar to the modification factor for single hadron spectra  $R_{AA}$ .

We have adjusted the energy loss parameter  $\epsilon_0$  to fit experimental data on both single ( $d\sigma_{AA}/dp_T dy$  between  $p_T = 4 - 20$  GeV/c) and away-side spectra [ $D_{AA}(z_T)$ ] in the most central Au + Au collisions at  $\sqrt{s} = 200$  GeV. The best fits occur for  $\epsilon_0 = 1.6 - 2.1$  GeV/fm as shown by the  $\chi^2$  in Fig. 3. The fact that both  $\chi^2$ 's reach their minima in the same region for two different measurements is highly nontrivial, providing convincing evidence for the jet quenching description.

Because of trigger bias, most of the contribution to dihadron spectra comes from dijets produced close and tangential to the surface of the overlapped region, as shown in Fig. 5. However, there are still about 25% of the contribution coming from dijets near the center of the overlapped region. These jets truly punch through the medium and emerge after finite amount of energy loss. This is why dihadron spectra is slightly more sensitive to

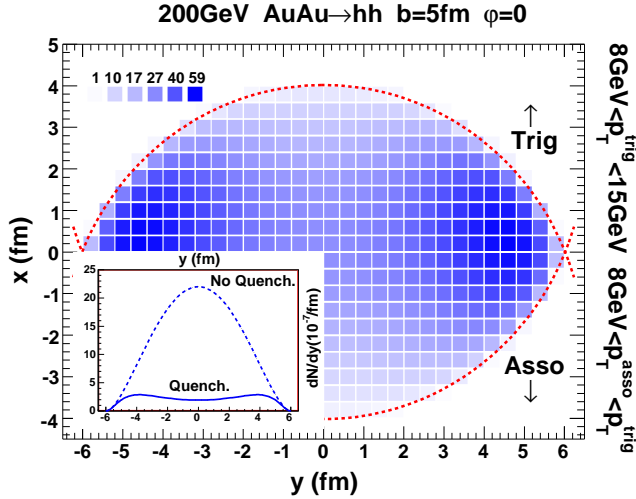


FIG. 5: The same as Fig. 2 except for dihadrons along the direction  $\phi = 0$  and  $\pi$ .

$\epsilon_0$  than the single spectra as was noted in Refs. [16, 17]. As one further increases the initial gluon density, the fraction of these punch-through jets will also diminish and the final dihadron spectra will be dominated by the tangential jets in the outer corona. Dihadron spectra at RHIC will also lose its sensitivity to the initial gluon density of the medium as shown in Fig. 3 Even if one includes the effect of transverse expansion of the bulk matter, the above results remain qualitatively the same [17].

Also shown in Fig. 3 are the single and dihadron suppression factors at the LHC energy as a function of  $\epsilon_0$  for fixed values of  $p_T^{\text{trig}} = 20$  GeV and  $p_T^{\text{asso}} = 10$  GeV. Because of the flattening of the overall spectra shape at the LHC energy, back-to-back dihadron spectra at a given  $p_T$  have more contribution from dijets with higher initial energy. They are therefore less suppressed than at the RHIC energy and are more sensitive to the initial gluon density. The single hadron spectra on the other

hand are increasingly dominated by surface emission and the suppression factor  $R_{AA}$  becomes much smaller than  $I_{AA}$  for dihadrons. From a model estimate of the bulk hadron production at LHC [12], the energy loss parameter is about  $\epsilon_0 \approx 5$  GeV/fm in central  $Pb + Pb$  collisions. The dihadron suppression factor  $I_{AA}$  at around this value of  $\epsilon_0$  is significantly larger than the single hadron suppression factor  $R_{AA}$  and is more sensitive to the initial gluon density.

In summary, we have used the NLO pQCD parton model with effective modified FF's due to radiative parton energy loss to study both single and dihadron spectra in high-energy heavy-ion collisions. We found that the surface emission dominates the single hadron production process within the range of initial gluon density in the most central  $Au + Au$  collisions at RHIC. However, there is still a significant fraction of dijets that are produced in the center of the dense medium and contribute to the final dihadron spectra after losing finite amount of energy. Therefore, dihadron spectra are more robust probes of the initial gluon density in the most central  $Au + Au$  collisions at RHIC while single hadron spectra become less sensitive. A simultaneous  $\chi^2$ -fit to both the single and dihadron spectra can be achieved within a narrow range of the energy loss parameters  $\epsilon_0 = 1.6 - 2.1$  GeV/fm. If the initial gluon density at RHIC were to increase further, dihadron spectra at a fixed  $p_T$  would also be dominated by the surface emission and become insensitive to the initial gluon density. At LHC, however, the flattening of the initial jet production spectra leads to an increase in the dihadron suppression factor. Dihadrons will therefore remain more robust probes within a large range of initial gluon density.

We thank P. Jacobs for helpful discussions. This work was supported by DOE under contracts DE-AC02-05CH11231 and DE-FG02-97IR40122, by NSFC under project Nos. 10440420018, 10475031 and 10635020, and by MOE of China under projects NCET-04-0744, SRFDP-20040511005 and CFKSTIP-704035.

- 
- [1] K. Adcox *et al.*, Phys. Rev. Lett. **88**, 022301 (2002); C. Adler *et al.*, Phys. Rev. Lett. **89**, 202301 (2002).
  - [2] C. Adler *et al.*, Phys. Rev. Lett. **90**, 082302 (2003).
  - [3] M. Gyulassy, I. Vitev, X.-N. Wang and B. W. Zhang, arXiv:nucl-th/0302077; A. Kovner and U. A. Wiedemann, arXiv:hep-ph/0304151, in *Quark Gluon Plasma 3*, editors: R.C. Hwa and X.-N. Wang, World Scientific, Singapore.
  - [4] K. J. Eskola, H. Honkanen, C. A. Salgado and U. A. Wiedemann, Nucl. Phys. A **747**, 511 (2005).
  - [5] J. F. Owens, Phys. Rev. D **65**, 034011 (2002); B. W. Harris and J. F. Owens, Phys. Rev. D **65**, 094032 (2002).
  - [6] X.-N. Wang, Phys. Lett. B **595**, 165 (2004); **579**, 299 (2004).
  - [7] B. A. Kniehl, G. Kramer and B. Potter, Nucl. Phys. B **582**, 514 (2000).
  - [8] M. Gyulassy, I. Vitev and X.-N. Wang, Phys. Rev. Lett. **86**, 2537 (2001).
  - [9] E. Wang and X.-N. Wang, Phys. Rev. Lett. **87**, 142301 (2001); **89**, 162301 (2002).
  - [10] C. A. Salgado and U. A. Wiedemann, Phys. Rev. Lett. **89**, 092303 (2002).
  - [11] H. L. Lai *et al.*, Eur. Phys. J. C **12**, 375 (2000).
  - [12] S. Y. Li and X.-N. Wang, Phys. Lett. B **527**, 85 (2002).
  - [13] H. Z. Zhang, J. Owens, E. Wang and X.-N. Wang, in preparation.
  - [14] Y. Akiba, Nucl. Phys. A **774**, 403 (2006); S. S. Adler, arXiv:nucl-ex/0611007.
  - [15] J. Adams *et al.*, Phys. Rev. Lett. **97**, 162301 (2006).
  - [16] A. Dainese, C. Loizides and G. Paic, Eur. Phys. J. C **38**, 461 (2005).
  - [17] T. Renk and K. J. Eskola, arXiv:hep-ph/0610059.